Microbial Ecology (2021) 81:134–145
https://doi.org/10.1007/s00248-020-01536-3

PLANT MICROBE INTERACTIONS

What Could Explain $\delta^{13}C$ Signatures in Biocrust Cyanobacteria of Drylands?

Eva Stricker[1] · Grace Crain[2] · Jenn Rudgers[1] · Robert Sinsabaugh[1] · Vanessa Fernandes[3,4] · Corey Nelson[3,4] · Ana Giraldo-Silva[3,4] · Ferran Garcia-Pichel[3] · Jayne Belnap[5] · Anthony Darrouzet-Nardi[2]

Received: 19 March 2020 / Accepted: 29 May 2020 / Published online: 3 July 2020

Abstract

Dryland ecosystems are increasing in geographic extent and contribute greatly to interannual variability in global carbon dynamics. Disentangling interactions among dominant primary producers, including plants and autotrophic microbes, can help partition their contributions to dryland C dynamics. We measured the $\delta^{13}C$ signatures of biological soil crust cyanobacteria and dominant plant species (C_3 and C_4) across a regional scale in the southwestern USA to determine if biocrust cyanobacteria were coupled to plant productivity (using plant-derived C mixotrophically), or independent of plant activity (and therefore purely autotrophic). Cyanobacterial assemblages located next to all C_3 plants and one C_4 species had consistently more negative $\delta^{13}C$ (by 2‰) than the cyanobacteria collected from plant interspaces or adjacent to two C_4 *Bouteloua* grass species. The differences among cyanobacterial assemblages in $\delta^{13}C$ could not be explained by cyanobacterial community composition, photosynthetic capacity, or any measured leaf or root characteristics (all slopes not different from zero). Thus, microsite differences in abiotic conditions near plants, rather than biotic interactions, remain a likely mechanism underlying the observed $\delta^{13}C$ patterns to be tested experimentally.

Keywords Carbon cycle · Biological soil crusts · Carbon stable isotopes · Chlorophyll · qPCR · Cyanobacteria

Introduction

Soil microbial activity is a major driver of global terrestrial carbon flux through decomposition, parasitic and mutualistic interactions with plants, and its influence on the productivity of autotrophs [1]. Determining the interactions between microbes and primary producers furthers our understanding of the controls on the C cycle and how these interactions may respond to future climate regimes [2, 3]. While much work has focused on how microbes contribute to plant productivity [4], less is known about how vascular plants contribute to the productivity of terrestrial autotrophic microbes and non-vascular organisms such as the cyanobacteria, algae, mosses, and lichens that, together with heterotrophic bacteria, fungi, and archaea, form surface biological soil crusts (biocrusts) [5]. Interactions between plant and autotrophic soil communities could range from direct resource transfers from plants to microbes [6] to indirect effects, such as litter material feeding autotrophs during decomposition, root respiration providing inorganic C, or plant individuals ameliorating abiotic stressors (e.g., reducing excess solar radiation through shading). In drylands, biocrusts may contribute ~ 1 Pg C yr^1 to global carbon uptake (reviewed in [7]), and this may be important to understand how drylands drive interannual variability in global C dynamics [8]. In addition, given that some cyanobacteria and cyano-lichens are important nitrogen fixers [9] and that biocrusts impact dryland hydrology [10], a better

Electronic supplementary material The online version of this article (https://doi.org/10.1007/s00248-020-01536-3) contains supplementary material, which is available to authorized users.

✉ Eva Stricker
evadr@unm.edu

[1] Department of Biology, University of New Mexico, Albuquerque, NM 87131, USA

[2] Department of Biological Sciences, University of Texas El Paso, El Paso, TX 79968, USA

[3] School of Life Sciences, Arizona State University, Tempe, AZ 85287, USA

[4] Center for Fundamental and Applied Microbiomics, Biodesign Institute, Arizona State University, Tempe, AZ 85287, USA

[5] US Geological Survey, Southwest Biological Science Center, Moab, UT 84532, USA

understanding of microbial C controls may also improve understanding of the N and water cycles.

Understanding how biocrust composition changes in relation to dominant vascular plants may show patterns that reflect plant-biocrust interactions. Biocrust composition varies across multiple scales. Biocrust communities range from moss/lichen-dominated biocrusts in cooler, moist regions, to cyanobacteria-dominated biocrusts in hotter, drier regions [11]. Even within cyanobacteria biocrust communities, variations in composition have been detected at the global [12], continental [13], and landscape scale [14] largely as a function of climate and edaphic conditions. Biocrust communities also vary at the microsite scale (dm) due to different moisture residence time across microtopographic aspects (e.g., NNW, ENE) [15]. Proximity to plants has yet to be evaluated in this respect, and biocrusted sites vary considerably in plant sizes and distance between plants, so one cannot deduce patterns that may indicate net direct or indirect influences of plants on biocrusts.

Resource transfers of C or nutrients are one potential direct interaction between plants and biocrusts, based on the tenet that a plant's excess C can be exchanged with biocrusts that control an important limiting resources such as fixed N [6, 16]. Despite contributing to C uptake at an annual scale [7], biocrusts as whole assemblages can show CO_2 release rates that exceed uptake rates under many observed conditions, although this effect is not seen when respiration is measured by O_2 export/import ratios [17]. If respiration indeed exceeds photosynthesis for prolonged periods in the biocrusts, mixotrophy of allochtonous C in the autotrophic biocrusts could be occurring to allow them to survive the unfavorable conditions. Previous work has shown that biocrusts (including both autotrophic and heterotrophic components) can take up both organic and inorganic forms of C [18], though subsequent biochemical uses within biocrust individuals' cells have not been disentangled. While cyanobacteria typically function as obligate autotrophs [19], biocrust cyanobacteria are able to both release and take up a large variety of organic compounds [20]. Indeed resource exchange interactions have been resolved in biocrust as an internal mechanism [21], but the existence, prevalence, or relative importance of such exchanges between plants and biocrusts remain to be determined.

Examination of stable isotopic signatures is one tool for determining sources and transfers of resources. In plants, stable isotopes of C reflect pathways of C fixation because C_3 plants lack the carbon-concentrating mechanisms present in C_4 plants. This causes C_3 plants to discriminate against ^{13}C more strongly, and thus they have lighter $\delta^{13}C$ signatures than C_4 plants. However, differences among plants in $\delta^{13}C$ can also be influenced by growth conditions, such as greater water availability, which tends to increase discrimination against ^{13}C [22, 23]. While much work has examined drivers of plant $\delta^{13}C$, few studies have determined $\delta^{13}C$ in surface microbial primary producers such as cyanobacteria [24, 25] or lichens [26], nor do we have a thorough understanding of what could drive the differences in $\delta^{13}C$, which range from − 24 to − 16‰ [24].

In our previous work, we showed that biocrust organisms next to a single species of C_3 plant (forb/subshrub *Guterrizia sarothrae*) had lighter $\delta^{13}C$ than organisms in interspaces, consistent with the hypothesis that biocrusts incorporate the relatively lighter C_3 plant-derived C when they are located near plants [27]. No differences in biocrust $\delta^{13}C$ values were observed between biocrusts near a single species of C_4 plant (grass *Bouteloua gracilis*) bases and those in interspaces, and no mechanisms for the observed variation in biocrust $\delta^{13}C$ values were evaluated. Four non-exclusive hypotheses may explain the observed patterns: (1) Biocrust communities differ taxonomically when adjacent to different plants versus in interspaces; (2) Biocrusts use organic C derived from living or dead plant tissues, and this plant C is more abundant near the plants than in interspaces. This mechanism suggests plant litter or exudate traits may correlate with biocrust $\delta^{13}C$ values; (3) Biocrusts access and use CO_2 present in the soil matrix for autotrophy, which may be isotopically light if it is enriched in plant root or plant rhizosphere-derived C, and thus differentially impact biocrusts close to plants. This mechanism suggests that root traits and rhizosphere activity may be correlated with biocrust $\delta^{13}C$ values; (4) Soils differ in their physicochemical characteristics in microsites adjacent to different plant bases versus interspaces between plants. Cool, moist conditions may be more favorable to prolonged photosynthetic activity and therefore result in different isotopic signature than photosynthetic activity under hotter, drier conditions. In any case, determining whether the mechanism underlying spatial variation in biocrust $\delta^{13}C$ values relates to resource exchange may be critical to understanding if plant-biocrust interactions affect biogeochemical cycling in drylands.

We sought to determine the importance of potential plant-biocrust resource exchanges and evaluate potential biological causes of spatial variation in biocrust $\delta^{13}C$ values. We considered that if the trend in biocrust $\delta^{13}C$ values near plants is found consistently in different areas and across different plant species, the trend is likely more biologically important. Thus, we collected biocrusts from different microsites across a regional gradient in the southwestern USA with two dominant C_3 plants and three dominant C_4 grasses to ask (Q1): do biocrusts growing in the interspaces between plants show different C isotope signatures than biocrusts growing adjacent to plants? Based on previous findings, we expected biocrusts near C_3 plant bases to show lighter signatures than those in the interspaces, but also that biocrusts near C_4 plants would not be different from those in the interspaces. To evaluate potential causes of any observed $\delta^{13}C$ differences, we asked (Q2) do characteristics of the biocrust cyanobacterial communities (richness, diversity, composition, relative abundance of taxa) correlate with observed $\delta^{13}C$ values? We first used PCR-based amplicon sequencing of the 16S rRNA gene. To

calculate the predicted community-weighted mean $\delta^{13}C$, we also measured stable isotope values of cultured cyanobacterial biocrust species to separate their basal autotrophic ^{13}C signatures from those of environmental samples that have the potential for mixotrophy. To address a potential plant-associated mechanism (Q3), we asked if plant leaf or root characteristics correlate with biocrust $\delta^{13}C$ signatures.

Methods

Unialgal Strains in DOC-Free Media

To determine relative differences in $\delta^{13}C$ signatures by cyanobacterial taxa commonly found in biocrusts, we obtained unialgal cultures of *Microcoleus vaginatus*, *M. steenstrupii*, *Tolypothrix* sp., *Nostoc* sp., *Scyotonema* sp., and *Schizothrix* sp. strains isolated from the Jornada Basin (JOR) in southern New Mexico. Cultures were grown in 15 mL of carbon-free liquid medium (variation of Ashbey's Medium: 0.2 g $CaCL_2 \cdot 2H_2O$, 0.2 g K_2HPO_4, 0.2 g $MgSO_4 \cdot 7H_2O$, 0.1 mL 10% MoO_3, 0.05 mL 10% $FeCl_3$, and 17 mM $NaNO_3$ in 1 L distilled H_2O) in 50 mL suspension culture flasks at room temperature (23 °C) with supplemental light (18.65–20.82 μE m^{-2} s^{-1}). Using DOC-free medium ensured that cyanobacteria incorporated only dissolved inorganic C. Growth in liquid culture likely changed how organisms interacted with CO_2 in the air compared to the cyanobacteria growing on the soil surface; $\delta^{13}C$ values of cultured cyanobacteria were less negative than those of free-living cyanobacteria likely because of reduced CO_2 diffusion through the liquid and low surface area for gas exchange for cyanobacteria that were clumped in the liquid. Additionally, cells that are fully hydrated may discriminate differently than cells that experience intermittent hydration and desiccation. A single replicate per strain (n = 1) was analyzed for $\delta^{13}C$. Samples were dried to constant weight and submitted for stable isotope analysis. We packed up to 5 mg of each sample in silver capsules (Costech Analytical Technologies Inc., Valencia, CA, USA), acid-fumigated them for 36 h to remove carbonates [28], then repacked them in tin capsules (Analytical Technologies Inc., Valencia, CA, USA) to improve combustion during analysis. Samples were analyzed at the Center for Stable Isotopes (University of New Mexico) on an ECS 4010 Elemental Analyzer and a Delta V Isotope Ratio Mass Spectrometer (Thermo Scientific, Waltham, MA, USA). Values were used with qPCR results (below) to determine the predicted community-weighted mean $\delta^{13}C$ value.

Field Sites

We sampled along a regional latitudinal gradient in the southwestern USA from the Colorado Plateau (COL) in southeastern Utah, the Sevilleta National Wildlife Refuge (SEV) in south-central New Mexico, to the Jornada Basin (JOR) in southern New Mexico (Table A1). The COL site is a cool desert ecosystem on the Upper Colorado Plateau. The SEV represents the transition between Chihuahuan Desert grassland and Colorado Plateau shrub-steppe. JOR is entirely Chihuahuan Desert grassland, with warmer winters characteristic of this ecosystem. Biocrusts are present at all three sites, with *Microcoleus*-dominated biocrusts at JOR and SEV and more diverse *Microcoleus* and *Collema* lichen biocrusts at COL [13]. Average rainfall days in JOR and SEV are ~ 7–9 events per month in monsoon season, whereas COL averages 5–6 events per month in both the spring and monsoon.

We selected target plant species that were dominant or common at a minimum of two of the sites and that represented different growth forms and photosynthetic pathways. We selected one target C_3 subshrub (*Guterrizia sarothrae*, all sites), one C_3 grass (*Achnatherum hymenoides*, COL, and SEV; JOR lacked a dominant C_3 grass), and 1-3 common C_4 grass species (*Bouteloua eriopoda*, SEV, and JOR; *B. gracilis*, COL, and SEV; and *Pleuraphis jamesii*, COL, and SEV; Table A1). Thus, we could investigate if the plant species identity was informative in explaining the biocrust $\delta^{13}C$, or if there were site by species differences.

Field Sampling, Processing, and Analysis

(Q1) To determine if biocrusts growing in different microsites have different C signatures, samples were collected in July–August 2016 except SEV *P. jamesii* which was collected Sep. 2018. Although the COL site tends to have early spring activity, we standardized collection time to the hot summer months. Temperature could affect $\delta^{13}C$ values, but by comparing within the same time of year for all target plant species × site combinations, we attempted to standardize collections at the higher temperatures experienced by the sites. Samples within each sites received ambient rainfall and rainfall cycles, and thus we were investigating the net effect of all the different times that the cyanobacteria were active. We collected paired samples of biocrusts, one from the base of each target plant (distance = 0 cm), and the other from the interspace (distance = 25 cm from the base of the target plant), with 12 target plant replicates per species (n = 12). For each sample, we collected and combined 6–8 independent subsamples of ~ 25 cm^2 to a depth of biological aggregation of the soil (0.5–1.0 cm) from multiple locations in all directions radiating around the base of the plant at each distance, ensuring that no other aboveground tissues of target or other adjacent plants were within 25 cm of any collection point. We avoided moss-only biocrusts and patches of plant litter.

Samples were homogenized and approximately 1 g was subsampled for chlorophyll content (methods described below) while the remainder was used to isolate active cyanobacteria. We wet each biocrust sample and picked out

cyanobacterial filaments under 10–20× magnification using forceps. Each filament was rinsed thoroughly in DI water then dried [27]. We cannot exclude the possibility that our washed cyanobacterial filaments included heterotrophic bacterial "cyanosphere" communities [21] (Fig. A2), but those components represent a very minor proportion of the total biomass.

Samples were packed for stable isotope analyses as above. Samples from JOR and COL were analyzed in the EaSI Lab in the Department of Geological Sciences at the University of Texas at El Paso, in which samples were combusted using a Pyrocube (Elementar, Langenselbold, Germany), followed by isotope analysis with a continuous-flow isotope ratio mass spectrometer (IsoPrime GeovisION, Elementar, Langenselbold, Germany). Samples from SEV were analyzed at the Center for Stable Isotopes (University of New Mexico). All carbon values were reported relative to the standard Pee Dee Belemnite. We excluded samples with < 0.3 mg of filaments because the peaks on the mass spectrometer were too low to be reliable; for biocrusts taken adjacent to *G. sarothrae* at JOR, this excluded all but one sample, reflecting low cyanobacterial abundance in the sandy microsite where the *G. sarothrae* was found.

We used linear mixed effects models for cyanobacteria $\delta^{13}C$ by distance (0 cm and 25 cm from plant base; categorical fixed effect) interacting with plant species with target plant individual and site as random effects. When there were significant interactions, we used FDR-corrected post-hoc analyses of each plant species separately and looked for differences by distance interacting with site. An additional post-hoc analysis was done for a subset of plant species with differences at $P < 0.10$ in $\delta^{13}C$ between 0 cm and 25 cm (Table A3).

(Q2) To determine cyanobacterial community composition, we aggregated and mixed ~ 10 g of biocrust soil from distance = 0 cm or distance = 25 cm from a random subset of five of the twelve paired replicates. Thus, we did not have the power to analyze the effects of target species × site. We submitted samples for sequencing at the Arizona State University Microbiome Analysis Laboratory (Tempe, AZ, USA) using methods reported in [29]. Briefly, DNA was extracted from 0.25 g of each sample with Qiagen Power Soil DNA extraction kit (Qiagen Inc. Germantown, MD, USA). We determined concentration with fluorometry (Qubit, Life Technologies, NY, USA) and used triplicate quantitative real-time PCR (qPCR) with the Sso Fast mix (Tio-rad, Hercules, CA, USA). The copies of 16S genes using the primer set 338F (GTGCCAGCMGCCGCGGTAA) and 518R (GGACTACHVGGGTWTCTAAT) were used to calculate total population sizes from qPCR. The 16S rRNA library was generated with the MiSeq Illumina platform using the V4 region with the primer set 515F and 806R [30]. Triplicates of PCR amplifications were pooled, quantified, purified, diluted, and quantified, then loaded in the sequencer using chemistry version 2 to generate 2 × 150 paired-end sequences.

The Qiime2 [31] bioinformatics pipeline was used for paired sequences. Reads had primers removed and were denoised, paired, trimmed to 150 base pairs and assembled using DADA2. Sequences were classified using Greengenes 13.8 [32] as the reference database to pick OTUs. Raw sequence data are available through NCBI (SRA number SUB5948515). All OTUs assigned to cyanobacteria or plastids were compared with the Cydrasil cyanobacteria database [33]. Sequences were aligned to the reference tree using RaxMLB algorithm [34] and visualized with iTOL3 server [35]. Singletons and doubletons were removed when they only occurred in a single sample [36].

We compared cyanobacterial sequence abundance from qPCR (natural log transformed) and cyanobacterial composition using PERMANOVA [37], with distance, species, and distance × species in linear models, and due to our bulked sampling design, we used sites as replicates.

To assess if the biocrust community composition was related to biocrust $\delta^{13}C$, we compared observed cyanobacterial $\delta^{13}C$ values to cyanobacterial diversity and richness, each interacting with plant species. Due to the bulked sampling design, linear models included sites as replicates.

We calculated the predicted community $\delta^{13}C$ values using the community-weighted mean $\delta^{13}C$ value of the single strains grown in unialgal culture. Although the absolute value of $\delta^{13}C$ is not directly comparable between culture conditions and field conditions due to environmental influences on $\delta^{13}C$ (aka, we do not expect the correlation to fall on the 1:1 line), we related predicted $\delta^{13}C$ × plant species to observed cyanobacterial $\delta^{13}C$ values with site as replicates.

To compare photosynthetic capacity among biocrusts, we extracted chlorophyll *a* using a single DMSO extraction [38]. Samples were left to extract for 3 days at room temperature in the dark. We calculated chlorophyll *a* content per g by absorbance at 665 nm on a Synergy H1 Hybrid plate reader (Biotek, Winooski, VT, USA) with 750 nm as a reference wavelength [38]. Higher concentration of photosynthetic machinery in the soil may drive less intense fractionation, as seen with leaves [39]. To compare potential photosynthetic capacity to observed $\delta^{13}C$ values, we used chlorophyll content × plant species as predictors and observed cyanobacterial $\delta^{13}C$ values in a mixed effect linear model with site and target plant individual as a random effect.

(Q3) If biocrusts use living plant-derived C, then the $\delta^{13}C$ of leaves and biocrusts should be positively correlated. Ten leaves were collected from each target plant ($n = 12$ for each plant species). All leaf samples were dried at 60 °C for 3 days, ground using liquid nitrogen and mortar and pestle, and ~ 4 mg were placed into tin capsules and submitted to stable isotope facilities as above.

If biocrusts on the soil surface intercept root-respired CO_2 from deeper soil rather than or in addition to atmospheric CO_2, then the density of roots should correlate with biocrust $\delta^{13}C$.

Root respiration can be > 40% of total soil respiration [40], and would have a $\delta^{13}C$ signature similar to the plant photosynthetic pathway. To compare density of plant roots by distance from plant, we selected three target individuals of each plant species. We pooled five soil (1.9 cm diameter, 5 cm depth) cores each from 0 cm and 25 cm from the base of each plant. Samples were sieved with 2-mm and 1-mm sieves, and roots were collected and washed. Roots were dried for 3 days at 60 °C and weighed. We could not determine if roots were attached to the target plant or were from neighboring plants.

We used linear mixed effects models of cyanobacteria $\delta^{13}C$ by leaf $\delta^{13}C$ × plant species with site as a random effect. We used root density × plant species as predictors and observed cyanobacterial $\delta^{13}C$ values in a mixed effect linear model with site as a random effect. Differences in cyanobacterial composition, biocrust chlorophyll *a* content, and root density by distance × plant species are presented in Table A4.

Results

(Q1) Biocrusts near both C_3 (A. hymenoides, G. sarothrae) and one C_4 (P. jamesii) plant species were depleted in $\delta^{13}C$ compared to paired biocrusts in the interspaces. The $\delta^{13}C$ values of cyanobacteria adjacent to the C_3 plant species were depleted by ~ 2‰ relative to paired samples in the interspaces (Table 1, Fig. 1; 2/3 sites had data for C_3 plants), consistent with prior observations for *G. sarothrae* [27]. The same trend was found for biocrusts near the C_4 plant *P. jamesii* at both sites where it was a focal species (Table 1, Fig. 1). The cyanobacteria located adjacent to the bases of the two C_4 *Bouteloua* species at all sites showed no statistical differences in $\delta^{13}C$ values compared to the paired interspace values (Table 1, Fig. 1, post-hoc $P > 0.10$), again consistent with previous observations [27].

(Q2) Cyanobacteria community composition did not differ with distance from plants. Composition of biocrusts differed by plant species (pseudo-$F_{4,10} = 2.44$, $P = 0.010$) but not by distance from plants (pseudo-$F_{1,10} = 0.45$, $P = 0.801$, species × distance pseudo-$F_{4,10} = 0.09$, $P = 0.945$, Fig. 2). Communities associated with *B. gracilis* and *G. sarothrae* were similar to each other and were all collected from within ~ 250 m of each other at SEV and ~ 300 m of each other at COL. Cyanobacteria collected near *B. eriopoda* at SEV tended to be less diverse than those collected near the other plant species, even though they were collected within ~ 250 m of the other species (Table A2). Communities associated with *P. jamesii* and *A. hymenoides* were similar in composition at COL and were collected within ~ 300 m of each other. Communities had low abundance and diversity near *A. hymenoides* at SEV. We observed that the soils where *A. hymenoides* were found were sandier than the soils with the other four plant species at the SEV. Soils near *G. sarothrae* at JOR yielded almost no cyanobacterial filaments and therefore were not sequenced.

Compositional differences or Chl *a* concentration did not account for differences in biocrust $\delta^{13}C$ between plant and interspace microsites. Cyanobacterial diversity did not correlate with the observed $\delta^{13}C$ value for any plant species (slope not different from zero; Table 2, Fig. 3). Cyanobacterial richness was overall negatively related to biocrust $\delta^{13}C$ (slope = − 0.41 ± 0.14 standard error [SE], $N = 20$), but this was driven by relationships of biocrusts collected near *B. gracilis* (slope = − 1.3 ± 0.4 SE, $n = 4$), *A. hymenoides* (slope = − 0.78 ± 0.29 SE, $n = 4$), and *G. sarothrae* (slope = − 1.05 ± 0.38 SE, $n = 4$) while biocrusts collected near *P. jamesii* had a positive slope (0.43 ± 0.19 SE, $n = 4$), and biocrusts collected near *B. eriopoda* had a slope not different from zero (0.62 ± 0.29 SE, $n = 4$).

The predicted value of biocrust $\delta^{13}C$ based on a community-weighted means did not correlate with the observed $\delta^{13}C$ value for any plant species (slope not different from zero; Table 2, Fig. 3). There was considerable variability in $\delta^{13}C$ of cyanobacterial strains grown in DOC-free media, both across taxa, within genera, and within strains (Table 3). The $\delta^{13}C$ value from cultures tended to be relatively heavier (aka, less negative $\delta^{13}C$ values) than that of samples observed in the field ([24]; non-zero intercept in Fig. 3c), suggesting

Table 1 Results from general linear mixed effects models testing for effects of distance from the target plant (0 cm = adjacent to plant base, 25 cm = interspace; categorical) and target plant species on observed $\delta^{13}C$ and post-hoc comparisons of each plant species separately including site (JOR, SEV, COL) as a main effect. *P* values ≤ 0.10 are in italics or < 0.05 are shown in bold

	All		*B. gracilis*		*A. hymenoides*		*G. sarothrae**		*P. jamesii*		*B. eriopoda*	
	X^2	*P*	X^2	*P*	X^2	*P*	X^2	*P*	X^2	*P*	X^2	*P*
Species	36.60	**<0.001**	*n.i.*		*n.i.*		*n.i.*		*n.i.*		*n.i.*	
Distance	22.68	**<0.001**	3.51	*0.061*	11.63	**<0.001**	8.66	**<0.003**	16.29	**<0.001**	0.00	0.976
Distance × Species	14.24	**0.001**	*n.i.*		*n.i.*		*n.i.*		*n.i.*		*n.i.*	
Site			34.27	**<0.001**	18.31	**<0.001**	36.22	**<0.001**	18.81	**<0.001**	8.90	**0.003**
Site × Distance			1.87	0.171	1.66	0.198	0.16	0.923	0.02	0.964	0.55	0.456

*Site = JOR distance = 0 had only 1 replicate. "*n.i.*" means "not included"

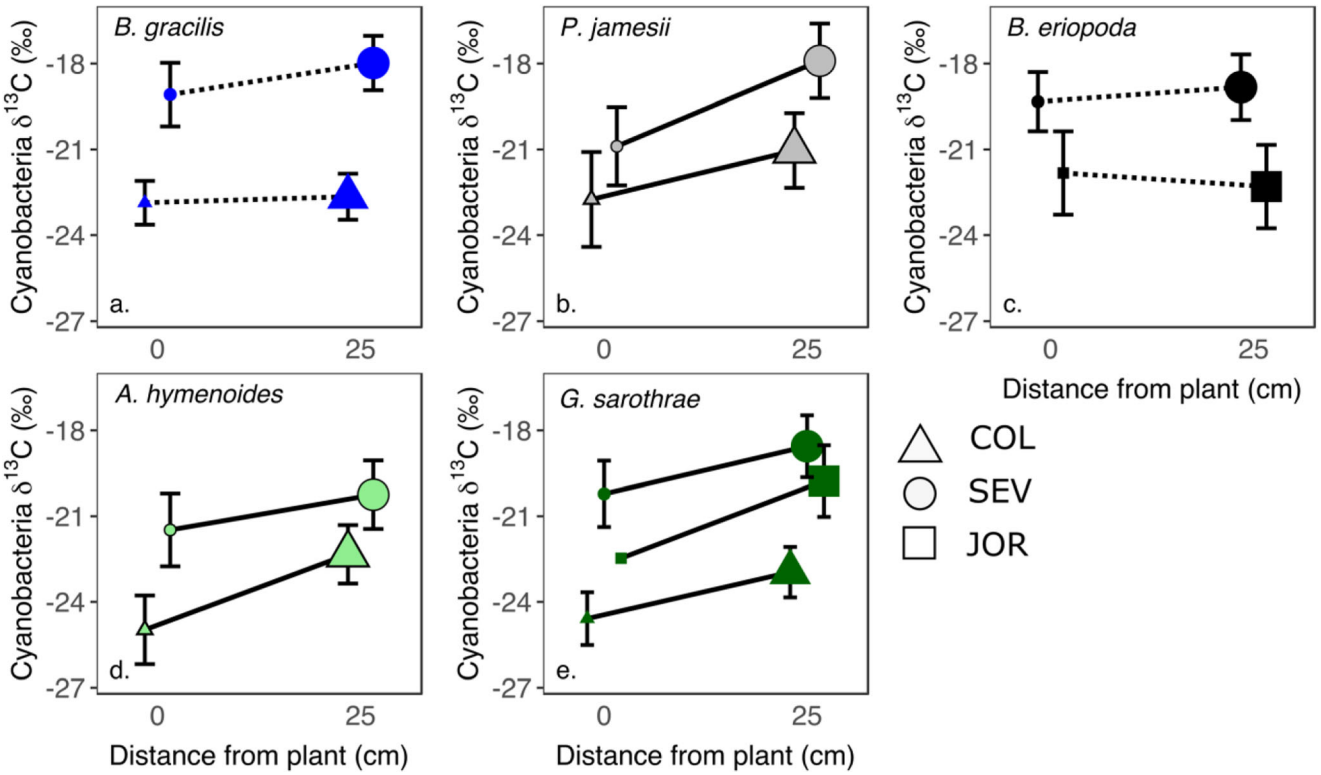

Fig. 1 Mean ± 95% CI of cyanobacteria $\delta^{13}C$ by distance from plant (categorical: 0 cm = adjacent to plant base, 25 cm = interspace) for C_4 target plants (**a** *B. gracilis*, **b** *P. jamesii*, **c** *B. eriopoda*) and C_3 target plants (**d** *A. hymenoides*, **e** *G. sarothrae*). Symbol color shows target plant species, size shows distance from plant, and shape shows sites (triangle = COL, circle = SEV, square = JOR). Solid lines show significant interactions between species and distance while dashed lines show non-significant relationships

that cyanobacteria in culture may have been more strongly CO_2 limited. Values were lighter than those reported in [25] with both DOC- and N-free media.

Chlorophyll *a* concentration (a proxy for photosynthetic capacity) did not explain the $\delta^{13}C$ signature of biocrusts because there was no relationship between chlorophyll *a* content and $\delta^{13}C$ value (Table 2, Fig. 3).

(Q3) Biocrust $\delta^{13}C$ values near plants did not reflect plant $\delta^{13}C$ values or root density. For COL and SEV, there was no relationship between leaf $\delta^{13}C$ and cyanobacteria $\delta^{13}C$ (Leaf $X^2 = 0.25$, $P = 0.613$; Species $X^2 = 2.39$, $P = 0.664$; Leaf × Species $X^2 = 1.95$, $P = 0.744$), but there was little variability within plant species (range ~ 4‰ within a type of photosynthetic pathway) relative to the variability among cyanobacteria (5–8‰). Root density did not explain the differences we observed in the cyanobacterial $\delta^{13}C$ near *G. sarothrae*, *A. hymenoides*, or *P. jamesii* (Table 2, Fig. 3) because although root density did differ by species and distance (Table A4), there was no significant relationship between biocrust $\delta^{13}C$ and root density for any species.

Discussion

We found continued support for the pattern that biocrust $\delta^{13}C$ is depleted near C_3 plants compared to interspaces between plants [27] across regional drylands of the southwestern US. We additionally found a similar signal with the previously unexamined C_4 plant *P. jamesii*. We used observational evidence to reject several possible mechanisms for these spatial differences in biocrust $\delta^{13}C$ relating to biocrust traits and plant traits (Table 1, Fig. 3). Although biocrust cyanobacterial communities and photosynthetic capacities differed among the adjacent plant species (Table A2), there were not strong relationships between community-weighted mean or chlorophyll *a* and biocrust $\delta^{13}C$, suggesting that the observed spatial variation in biocrust $\delta^{13}C$ was not caused by these characteristics of the biocrusts. If biocrust cyanobacteria were using mixotrophy, we would have seen systematic differences in $\delta^{13}C$ values with distances from plant species with different types of photosynthetic pathway. The observed patterns in biocrust $\delta^{13}C$ near C_3 plants vs. interspaces are consistent with the hypothesis that there were differences in availability of $\delta^{13}C$-depleted plant-derived C that was taken up by cyanobacteria, either as organic C or respired C. However, the C_4 *P. jamesii* trend suggests that the differences in biocrust $\delta^{13}C$ are not solely due to plant litter/exudates/respiration because the biocrust $\delta^{13}C$ near the *P. jamesii* should have been *heavier* than the interspace values rather than lighter. Although there were differences in rooting density by distance from the plant base, and different plant species had different

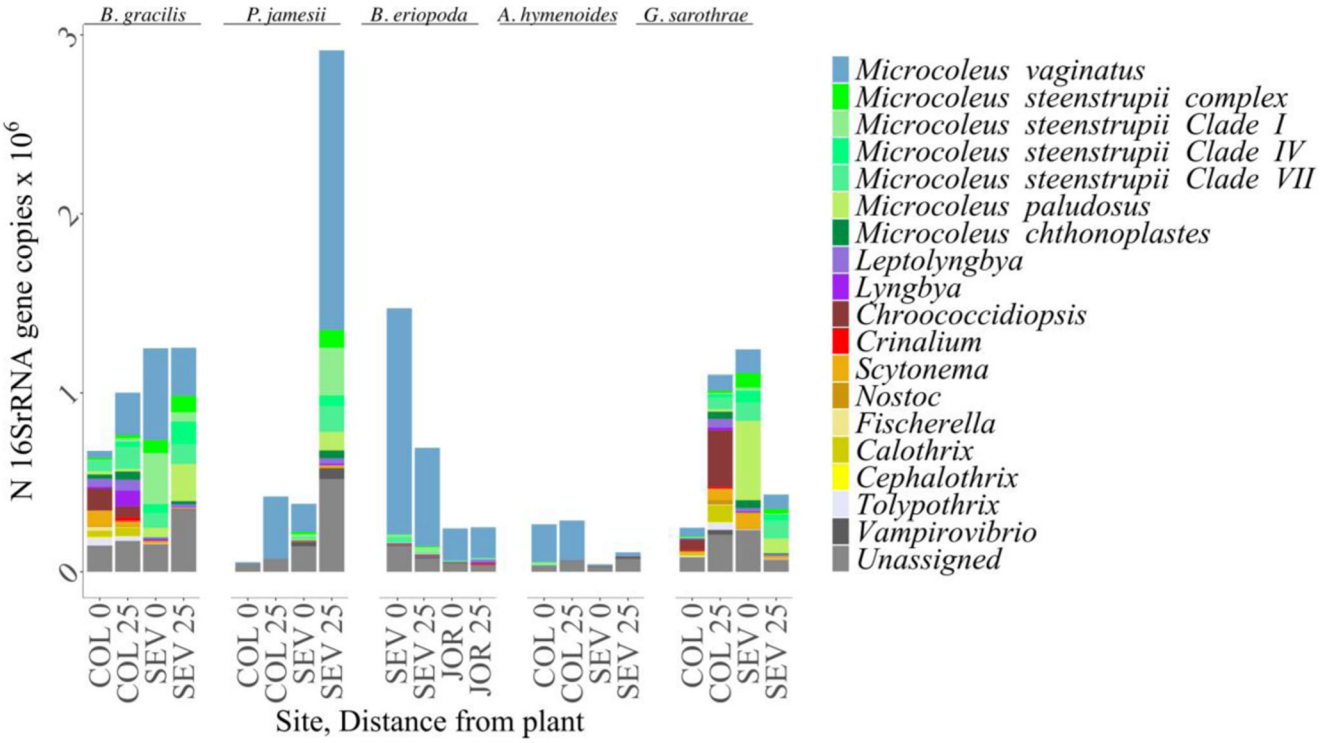

Fig. 2 Cyanobacterial abundance by taxa with target plant species (label above facets: *B. gracilis*, *P. jamesii*, *B. eriopoda*, *A. hymenoides*, and *G. sarothrae*) at three sites (COL, SEV, JOR) and distance from plant (0 cm = adjacent to plant base, 25 cm = interspace) as determined by high-throughput 16S rRNA gene analyses coupled to q-PCR. Phylogenetic assignments for each OTU were based on blast to the Cydrasil database, and carried to the genus or species level, as feasible

$\delta^{13}C$ value, these traits were not strongly correlated with biocrust $\delta^{13}C$, suggesting that the observe spatial variation in $\delta^{13}C$ was not caused by above or belowground litter and/or exudates of the plants.

Biogeographic patterns in biocrust composition across our regional survey were largely consistent with previous observations [13] but did not explain microsite differences in biocrust $\delta^{13}C$. Specifically, we found *M. vaginatus* abundant in most COL samples and the *M. steenstrupii* complex to be dominant or abundant at SEV. The two aggregated JOR samples were dominated by *M. vaginatus*, an unexpected result given Garcia-Pichel et al.'s (2013) results on the heat intolerance of *M. vaginatus*, but with only two samples, it is difficult to draw strong conclusions. Biocrust composition did not explain the trends in cyanobacterial $\delta^{13}C$ values by distance from plant because there were not consistent differences in composition by distance from plant. The predicted $\delta^{13}C$ values may have been overly simplistic calculations because previous work has shown that higher microbial community complexity is related to higher $\delta^{13}C$ discrimination [41]. This is consistent with the more diverse samples associated with *B. gracilis* and *G. sarothrae* (Table A4) having lower

Table 2 Results from general linear mixed effects models testing for biocrust characteristics (cyanobacterial diversity, rarefied species richness, predicted $\delta^{13}C$, and chlorophyll *a* μg g^{-1} soil) and plant characteristics (leaf $\delta^{13}C$ and root density g cm^{-3} soil) and plant species on observed cyanobacteria $\delta^{13}C$. *P* values ≤ 0.05 are shown in bold

	Cyanobacteria Diversity		Cyanobacteria species richness		Predicted cyanobacteria community $\delta^{13}C$		Chlorophyll *a*		Leaf $\delta^{13}C$		Root density	
	F	*P*	*F*	*P*	X^2	*P*	*F*	*P*	X^2	*P*	X^2	*P*
Predictor	0.60	0.458	6.50	**0.029**	1.30	0.253	3.21	*0.073*	0.04	0.847	0.06	0.805
Species	1.58	0.253	7.30	**0.005**	3.65	0.456	11.58	**0.021**	4.12*	0.390	6.10	0.192
Predictor × Species	1.46	0.284	8.88	**0.002**	3.70	0.448	3.70	0.448	4.71	0.319	5.25	0.263

*Excludes *P. jamesii* from SEV and *B. eriopoda* from JOR because leaf samples and biocrust samples were collected from different plants.

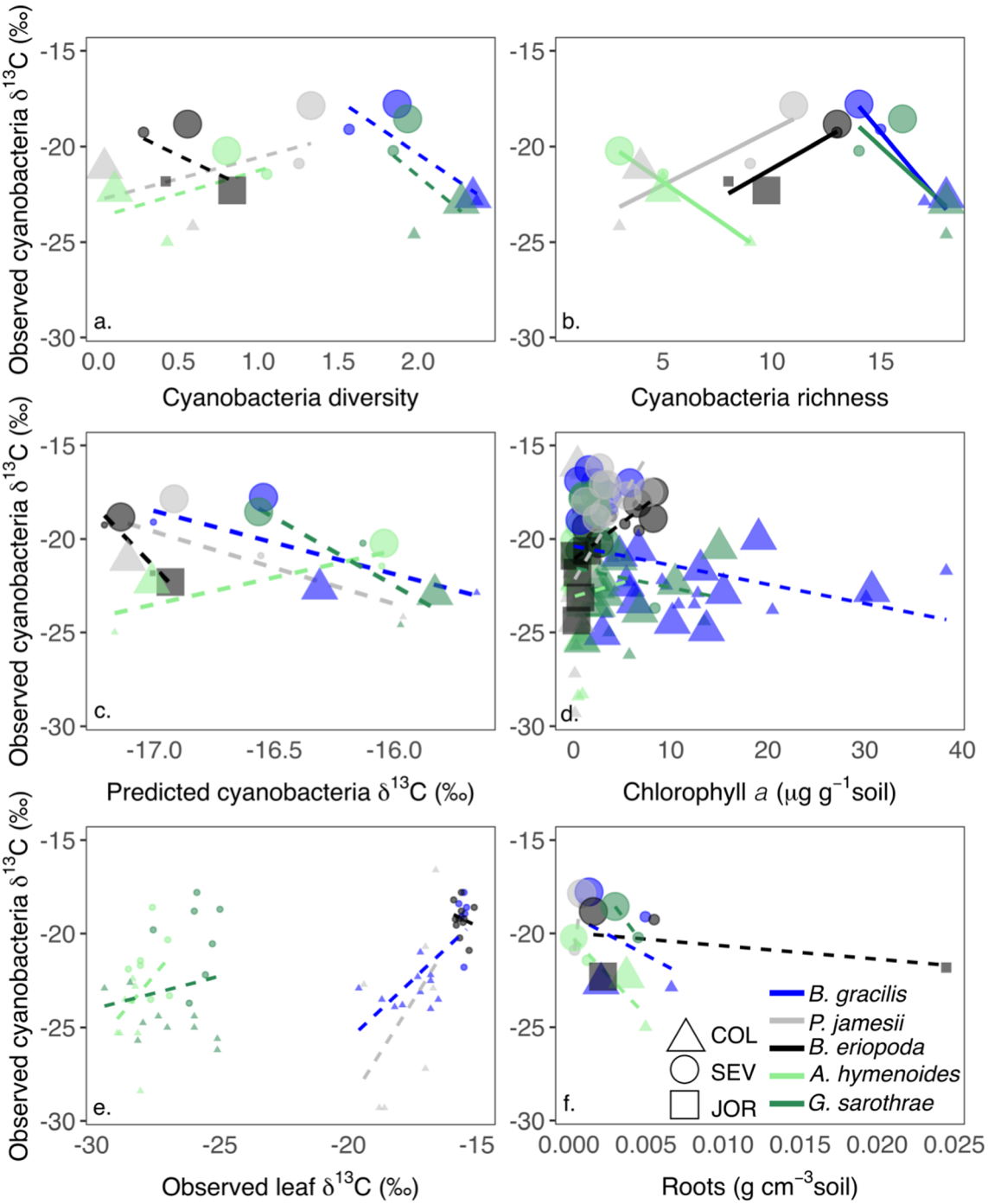

Fig. 3 Mean (**a**, **b**, **c**, **f**), or raw values (**d**, **e**) of field-collected, cleaned cyanobacteria filament $\delta^{13}C$ by characteristics of biocrusts (**a** cyanobacterial diversity and **b** rarefied species richness from 16S rRNA gene analyses coupled to q-PCR; **c** predicted $\delta^{13}C$ from the community weighted mean from unialgal strains plus relative frequency from 16S rRNA gene analyses; and **d** chlorophyll *a* content) and plants (**e** observed leaf $\delta^{13}C$ and **f** root density) by target plant species. Symbol and line color show target plant species (blue = *B. gracilis*, grey = *P. jamesii*, black = *B. eriopoda*, light green = *A. hymenoides*, and dark green = *G. sarothrae*); solid lines show significant interactions between plant species and predictor on observed cyanobacteria filament $\delta^{13}C$ and dashed lines show non-significant relationships. Shape shows sites (triangle = COL, circle = SEV, square = JOR) which was included as a random effect in the models (Table 3). Although distance from plant was not included in models, size shows distance from plant for consistency with Fig. 1 (small = 0 cm, large = 25 cm)

$\delta^{13}C$ values. These results still do not explain the patterns of differences in cyanobacteria by distance from specific plant taxa. Better estimates of mixed biocrust filament $\delta^{13}C$ values could be produced by creating model communities with varying richness and composition recording the $\delta^{13}C$ values of constructed communities, which could be beneficial to

Table 3 %C and $\delta^{13}C$ of unialgal cultures of cyanobacteria taxa with strain origin, and NCBI accession number, Genbank submission number, and which groups the $\delta^{13}C$ value was used for in the community-weighted means (see Figs. 2 and 3).

	Strain origin	NCBI	Genbank	%C	$\delta^{13}C$	Groups that used the given $\delta^{13}C$ value
Tolypothrix sp. sample	JOR	MK487660	SUB4485019	25.9	-13.1	*Tolypothrix*
Scytonema sp. sample	JOR	MK487672	SUB4485019	20.4	-14.5	*Scytonema*
Schizothrix sp. sample	JOR	MK487699	SUB4485019	19.4	-15.1	*Not used*
Nostoc sp. sample	near JOR	MK487651	SUB4485019	25.4	-16.0	*Nostoc*
Microcoleus steenstrupii	JOR	MK487677	SUB4485019	27.8	-17.3	*Microcoleus_steenstrupii_complex, Microcoleus_steenstrupii_Clade_I, Microcoleus_steenstrupii_Clade_IV, Microcoleus_steenstrupii_Clade_VII*
Microcoleus vaginatus	JOR	MK487635	SUB4485019	25.6	-17.4	*Microcoleus_vaginatus*
Average					-15.7	*Calothrix, Cephalothrix, Chroococcidiopsis, Crinalium, Fischerella, Leptolyngbya, Lyngbya, Microcoleus_chthonoplastes, Microcoleus_paludosus, Unassigned, Vampirovibrio*

understand the mechanisms of community level carbon cycling in biocrusts and therefore to build robust communities for restoration activities.

We did not find evidence for mixotrophy based on plant-derived C in the biocrust cyanobacterial community and thus did not find support for resource exchange interactions between dryland primary producers. It is well-known that plant and interspace microsites tend to differ in resource availability and microbial abundance, with an elevated "fertile island" effect in dryland systems [42, 43] (Appendix A5). We did not find differences in biocrust cyanobacteria composition by distance from any target plant species, but did find differences in C signature by distance from some plants, suggesting that metabolic activities differ. The microbes found adjacent to plants versus those in interspaces should have access to different substrates, from labile recently-fixed C leaked or exuded from plant roots to more recalcitrant soil organic material or litter [44]. $\delta^{13}C$ values in litter and decaying soil organic material reflect the living plant community signatures [45, 46] and thus can be used to identify C sources. Microorganism communities have been shown to use considerable plant-derived C (20–50% in agricultural fields) in addition to bulk soil organic material, and different groups (Gram-positive vs. Gram-negative) use different C sources [47]. Many cyanobacteria can be facultative heterotrophs [48], incorporating sugars to support growth, but there has been little evidence that they incorporate C from complex plant litter under field conditions [49, 50]. Green et al. [18] investigated ^{13}C-glutamate transfer from plants to biocrusts and found considerable transfer within 4 days. However, the cyanobacteria were not separated from the bulk soil, and thus it was not determined that this was evidence of mixotrophy in the cyanobacteria or if the heterotrophic components in the soil were retaining the glutamate. Although the proposed transfer is possible, we did not find consistent trends in cyanobacteria $\delta^{13}C$ values by the widespread, dominant C_4 plants, and thus the transfer is likely not biologically important.

To understand the drivers of spatial variation in biocrust $\delta^{13}C$, several hypotheses remain to be tested. First, there may be differences in abiotic characteristics associated with different target plant species that vary with distance from the plant. Access to water is associated with C isotope discrimination in plants [51] and thus plants from microsites that differ in water availability show differences in C signature. We found this pattern at the regional scale: *B. gracilis* and *G. sarothrae* at SEV (drier) had higher leaf $\delta^{13}C$ than those species at COL (wetter). This pattern has also been observed in non-plant autotrophs: in cyanobacteria and lichen communities in field conditions in tropical dry and wet savannas, microsites with higher soil moisture or water retention seemed to be more important in determining $\delta^{13}C$ than the dominant microbial taxa [24]. In our study sites, we observed that *G. sarothrae* produced denser shade and often accumulated litter under the canopy that could affect surface light availability, temperature, moisture, and soil chemistry more than the grasses. *A. hymenoides* has longer leaves than the C_4 grasses and may have a stronger influence on air movement near the surface which could lead to higher relative humidity during windy conditions than plants with shorter leaves. Preliminary data supports abiotic differences by plant taxa, with cooler daily mean and maximum temperatures under *G. sarothrae* than in the nearby interspaces compared or under any grass species (Appendix A6). To determine if hypothesized differences in temperature, moisture, soil chemistry, or soil structure can account for the observed ~ 2‰ differences in cyanobacterial filaments in different microsites, direct manipulation of temperature, moisture (including wet-dry cycles),

and other soil physical and chemical response curves (including potentially non-linear relationships) would be needed, which was outside the scope of this study.

Conclusions

Our study does not support the hypothesis that living plant C, plant litter, or root-density correlated C is becoming integrated into cyanobacterial tissue, and thus we did not find support for the hypothesis that plants may exchange C for biocrust-derived N via soil fungi [6]. Our study does not support the hypothesis that living plant C, plant litter, or root-density correlated C is becoming integrated into cyanobacterial tissue. Thus, plant-microbe interactions may be more driven by habitat amelioration than by resource exchanges. Manipulative experiments in controlled lab and field conditions are needed to further disentangle the drivers in biocrust C characteristics.

Understanding whether carbon transfer could be a potential resource-mediated interaction between plants and microbes may enhance understanding of biogeochemical cycling in these systems. However, plants and biocrusts occur across a much wider range of conditions than we encompassed in this study and so conclusions from our study do not rule out resource transfer in other systems. Relating biocrust C dynamics to dryland community and ecosystem function across broader scales is critical for predicting biogeochemical cycling at global scales.

Acknowledgments We thank Jarek Kwiecinski, Noelle Martinez, Laura Green, Charlie Mettler, Vishwa Patel, Maria Isabel Siles Asaff, for lab and field work assistance. We thank Dr. Benjamin Brunner at UTEP and Laura Burkemper, Seth Newsome, and Viorel Atudorei for stable isotope analysis assistance.

Availability of Data and Material Data is available from EDI (https://doi.org/10.6073/pasta/b59b733653671fc1a28f12a865e121bc) and sequences are available at NCBI (SRA number SUB5948515).

Authors' Contributions ES, JR, RS, FG-P, JB, and AD-N made substantial contributions to the conception or design of the work; GC, VF, CN, AG-S contributed acquisition, analysis, and interpretation of data; all contributed to drafting the work and revisions.

Funding Information Funding was provided by NSF nos. 1557135, 1557162, and Jornada LTER grant nos. 1832194. This research was partially supported by grants from the National Science Foundation to the University of New Mexico for Long-term Ecological Research (SEV-LTER).

Compliance with Ethical Standards

Conflict of Interest The authors declare that they have no conflict of interest.

Ethics Approval Not applicable

Consent to Participate Not applicable

Consent for Publication Not applicable

Code Availability Code is available at https://github.com/evadeeter/cyanobacteria-13C.

References

1. Jackson RB, Lajtha K, Crow SE et al (2017) The ecology of soil carbon: pools, vulnerabilities, and biotic and abiotic controls. Annu Rev Ecol Evol Syst 48:419–445. https://doi.org/10.1146/annurev-ecolsys-112414-054234
2. Bardgett RD, Wardle DA (2010) Aboveground-belowground linkages: biotic interactions, ecosystem processes, and global change. Oxford University Press, Oxford, New York
3. Classen AT, Sundqvist MK, Henning JA et al (2015) Direct and indirect effects of climate change on soil microbial and soil microbial-plant interactions: What lies ahead? Ecosphere 6:130. https://doi.org/10.1890/ES15-00217.1
4. van der Heijden MGA, Bardgett RD, van Straalen NM (2008) The unseen majority: soil microbes as drivers of plant diversity and productivity in terrestrial ecosystems. Ecol Lett 11:296–310. https://doi.org/10.1111/j.1461-0248.2007.01139.x
5. Zhang Z-S, Zhao Y, Dong X-J, Shi YF, Chen YL, Hu YG (2016) Evolution of soil respiration depends on biological soil crusts across a 50-year chronosequence of desert revegetation. Soil Sci Plant Nutr 62:140–149. https://doi.org/10.1080/00380768.2016.1165597
6. Rudgers JA, Dettweiler-Robinson E, Belnap J, Green LE, Sinsabaugh RL, Young KE, Cort CE, Darrouzet-Nardi A (2018) Are fungal networks key to dryland primary production? Am J Bot 105:1783–1787. https://doi.org/10.1002/ajb2.1184
7. Sancho LG, Belnap J, Colesie C, Raggio J, Weber B (2016) Carbon budgets of biological soil crusts at micro-, meso-, and global scales. In: Weber B, Büdel B, Belnap J (eds) Biological soil crusts: an organizing principle in drylands. Springer International Publishing, Cham, pp 287–304
8. Ahlström A, Xia J, Arneth A, Luo Y, Smith B (2015) Importance of vegetation dynamics for future terrestrial carbon cycling. Environ Res Lett 10:054019. https://doi.org/10.1088/1748-9326/10/5/054019
9. Elbert W, Weber B, Burrows S, Steinkamp J, Büdel B, Andreae MO, Pöschl U (2012) Contribution of cryptogamic covers to the global cycles of carbon and nitrogen. Nat Geosci 5:459–462. https://doi.org/10.1038/ngeo1486
10. Chamizo S, Canton Y, Lazaro R et al (2012) Crust composition and disturbance drive infiltration through biological soil crusts in semiarid ecosystems. Ecosystems 15:148–161. https://doi.org/10.1007/s10021-011-9499-6
11. Belnap J, Weber B, Büdel B (2016) Biological soil crusts as an organizing principle in drylands. In: Weber B, Büdel B, Belnap J (eds) Biological soil crusts: an organizing principle in drylands. Springer International Publishing, Cham, pp 3–13
12. Machado de Lima NM, Fernandes VMC, Roush D et al (2019) The compositionally distinct cyanobacterial biocrusts from Brazilian Savanna and their environmental drivers of community diversity. Front Microbiol 10. https://doi.org/10.3389/fmicb.2019.02798
13. Garcia-Pichel F, Loza V, Marusenko Y, Mateo P, Potrafka RM (2013) Temperature drives the continental-scale distribution of key microbes in topsoil communities. Science 340:1574–1577. https://doi.org/10.1126/science.1236404

14. Nagy ML, Perez A, Garcia-Pichel F (2005) The prokaryotic diversity of biological soil crusts in the Sonoran Desert (Organ Pipe Cactus National Monument, AZ). FEMS Microbiol Ecol 54:233–245. https://doi.org/10.1016/j.femsec.2005.03.011
15. Bowker MA, Belnap J, Davidson DW, Harland G (2006) Correlates of biological soil crust abundance across a continuum of spatial scales: support for a hierarchical conceptual model. J Appl Ecol 43:152–163. https://doi.org/10.1111/j.1365-2664.2006.01122.x
16. Collins SL, Belnap J, Grimm NB, Rudgers JA, Dahm CN, D'Odorico P, Litvak M, Natvig DO, Peters DC, Pockman WT, Sinsabaugh RL, Wolf BO (2014) A multiscale, hierarchical model of pulse dynamics in arid-land ecosystems. Annu Rev Ecol Evol Syst 45:397–419. https://doi.org/10.1146/annurev-ecolsys-120213-091650
17. Garcia-Pichel F, Belnap J (1996) Microenvironments and microscale productivity of cyanobacterial desert crusts. J Phycol 32:774–782
18. Green LE, Porras-Alfaro A, Sinsabaugh RL (2008) Translocation of nitrogen and carbon integrates biotic crust and grass production in desert grassland. J Ecol 96:1076–1085. https://doi.org/10.1111/j.1365-2745.2008.01388.x
19. Garcia-Pichel F (2009) Cyanobacteria. Encyclopedia of Microbiology. Elsevier, pp 107–124. https://www-sciencedirect-com.libproxy.unm.edu/science/article/pii/B9780123739445002509?via%3Dihub
20. Baran R, Brodie EL, Mayberry-Lewis J, Hummel E, da Rocha UN, Chakraborty R, Bowen BP, Karaoz U, Cadillo-Quiroz H, Garcia-Pichel F, Northen TR (2015) Exometabolite niche partitioning among sympatric soil bacteria. Nat Commun 6:8289. https://doi.org/10.1038/ncomms9289
21. Couradeau E, Giraldo-Silva A, De Martini F, Garcia-Pichel F (2019) Spatial segregation of the biological soil crust microbiome around its foundational cyanobacterium, Microcoleus vaginatus, and the formation of a nitrogen-fixing cyanosphere. Microbiome 7:55. https://doi.org/10.1186/s40168-019-0661-2
22. Dawson TE, Mambelli S, Plamboeck AH, Templer PH, Tu KP (2002) Stable isotopes in plant ecology. Annu Rev Ecol Syst 33:507–559. https://doi.org/10.1146/annurev.ecolsys.33.020602.095451
23. Diefendorf AF, Mueller KE, Wing SL, Koch PL, Freeman KH (2010) Global patterns in leaf 13C discrimination and implications for studies of past and future climate. Proc Natl Acad Sci 107:5738–5743. https://doi.org/10.1073/pnas.0910513107
24. Ziegler H, Lüttge U (1998) Carbon isotope discrimination in cyanobacteria of rocks of inselbergs and soils of savannas in the neotropics. Bot Acta 111:212–215
25. Darby BJ, Neher DA (2012) Stable isotope composition of microfauna supports the occurrence of biologically fixed nitrogen from cyanobacteria in desert soil food webs. J Arid Environ 85:76–78. https://doi.org/10.1016/j.jaridenv.2012.06.006
26. Lange OL, Kilian E, Ziegler H (1986) Water vapor uptake and photosynthesis of lichens: performance differences in species with green and blue-green algae as phycobionts. Oecologia 71:104–110
27. Dettweiler-Robinson E (2018) Biocrust carbon isotope signature was depleted under a C3 forb compared to interspace. Plant Soil 429:101–111. https://doi.org/10.1007/s11104-017-3558-5
28. Harris D, Horwáth WR, van Kessel C (2001) Acid fumigation of soils to remove carbonates prior to total organic carbon or CARBON-13 isotopic analysis. Soil Sci Soc Am J 65:1853–1856. https://doi.org/10.2136/sssaj2001.1853
29. Fernandes VMC, Machado de Lima NM, Roush D, Rudgers J, Collins SL, Garcia-Pichel F (2018) Exposure to predicted precipitation patterns decreases population size and alters community structure of cyanobacteria in biological soil crusts from the Chihuahuan Desert: Changing rainfall effects on soil cyanobacteria. Environ Microbiol 20:259–269. https://doi.org/10.1111/1462-2920.13983
30. Caporaso JG, Lauber CL, Walters WA, Berg-Lyons D, Huntley J, Fierer N, Owens SM, Betley J, Fraser L, Bauer M, Gormley N, Gilbert JA, Smith G, Knight R (2012) Ultra-high-throughput microbial community analysis on the Illumina HiSeq and MiSeq platforms. ISME J 6:1621–1624. https://doi.org/10.1038/ismej.2012.8
31. Bolyen E, Rideout JR, Dillon MR et al (2018) QIIME 2: Reproducible, interactive, scalable, and extensible microbiome data science. https://doi.org/10.7287/peerj.preprints.27295v2
32. DeSantis TZ, Hugenholtz P, Larsen N et al (2006) Greengenes, a Chimera-Checked 16S rRNA Gene Database and Workbench Compatible with ARB. Appl Environ Microbiol 72:5069–5072. https://doi.org/10.1128/AEM.03006-05
33. Roush D (2018) Fgplab/Cydrasil: V1.0.1-Zen. Zenodo
34. Stamatakis A (2014) RAxML version 8: a tool for phylogenetic analysis and post-analysis of large phylogenies. Bioinformatics 30:1312–1313. https://doi.org/10.1093/bioinformatics/btu033
35. Letunic I, Bork P (2016) Interactive tree of life (iTOL) v3: an online tool for the display and annotation of phylogenetic and other trees. Nucleic Acids Res 44:W242–W245. https://doi.org/10.1093/nar/gkw290
36. Allen HK, Bayles DO, Looft T, Trachsel J, Bass BE, Alt DP, Bearson SMD, Nicholson T, Casey TA (2016) Pipeline for amplifying and analyzing amplicons of the V1–V3 region of the 16S rRNA gene. BMC Res Notes 9:380. https://doi.org/10.1186/s13104-016-2172-6
37. Anderson MJ (2001) A new method for non-parametric multivariate analysis of variance. Aust Ecol 26:32–46. https://doi.org/10.1111/j.1442-9993.2001.01070.pp.x
38. Castle SC, Morrison CD, Barger NN (2011) Extraction of chlorophyll a from biological soil crusts: A comparison of solvents for spectrophotometric determination. Soil Biol Biochem 43:853–856. https://doi.org/10.1016/j.soilbio.2010.11.025
39. Soundararajan M (2012) Leaf chlorophyll levels influence carbon isotope discrimination in soybean and maize. Int J Biosci Biochem Bioinforma:207–211. https://doi.org/10.7763/IJBBB.2012.V2.102
40. Yevdokimov IV, Ruser R, Buegger F, Marx M, Munch JC (2007) Carbon turnover in the rhizosphere under continuous plant labeling with 13CO2: partitioning of root, microbial, and rhizomicrobial respiration. Eurasian Soil Sci 40:969–977. https://doi.org/10.1134/S1064229307090074
41. Yang W, Magid J, Christensen S, Rønn R, Ambus P, Ekelund F (2014) Biological 12C–13C fractionation increases with increasing community-complexity in soil microcosms. Soil Biol Biochem 69:197–201. https://doi.org/10.1016/j.soilbio.2013.10.030
42. Schlesinger WH, Pilmanis AM (1998) Plant-soil interactions in deserts. Biogeochemistry 42:169–187
43. Ochoa-Hueso R, Eldridge DJ, Delgado-Baquerizo M, Soliveres S, Bowker MA, Gross N, le Bagousse-Pinguet Y, Quero JL, García-Gómez M, Valencia E, Arredondo T, Beinticinco L, Bran D, Cea A, Coaguila D, Dougill AJ, Espinosa CI, Gaitán J, Guuroh RT, Guzman E, Gutiérrez JR, Hernández RM, Huber-Sannwald E, Jeffries T, Linstädter A, Mau RL, Monerris J, Prina A, Pucheta E, Stavi I, Thomas AD, Zaady E, Singh BK, Maestre FT (2018) Soil fungal abundance and plant functional traits drive fertile island formation in global drylands. J Ecol 106:242–253. https://doi.org/10.1111/1365-2745.12871
44. Börjesson G, Menichetti L, Thornton B, Campbell CD, Kätterer T (2016) Seasonal dynamics of the soil microbial community: assimilation of old and young carbon sources in a long-term field experiment as revealed by natural ^{13} C abundance: seasonal changes among microbes in agricultural soil. Eur J Soil Sci 67:79–89. https://doi.org/10.1111/ejss.12309
45. Liao JD, Boutton TW, Jastrow JD (2006) Organic matter turnover in soil physical fractions following woody plant invasion of

grassland: Evidence from natural 13C and 15 N. Soil Biol Biochem 38:3197–3210. https://doi.org/10.1016/j.soilbio.2006.04.004

46. Bai E, Boutton TW, Liu F, Wu XB, Hallmark CT, Archer SR (2012) Spatial variation of soil δ13C and its relation to carbon input and soil texture in a subtropical lowland woodland. Soil Biol Biochem 44:102–112. https://doi.org/10.1016/j.soilbio.2011.09.013
47. Kramer C, Gleixner G (2006) Variable use of plant- and soil-derived carbon by microorganisms in agricultural soils. Soil Biol Biochem 38:3267–3278. https://doi.org/10.1016/j.soilbio.2006.04.006
48. Rippka R, Deruelles J, Waterbury J et al (1979) Generic assignments, strain histories and properties of pure cultures of cyanobacteria. J Gen Microbiol 111:1–61
49. Bernard L, Mougel C, Maron P-A, Nowak V, Lévêque J, Henault C, Haichar FZ, Berge O, Marol C, Balesdent J, Gibiat F, Lemanceau P, Ranjard L (2007) Dynamics and identification of soil microbial populations actively assimilating carbon from ^{13}C-labelled wheat residue as estimated by DNA- and RNA-SIP techniques. Environ Microbiol 9:752–764. https://doi.org/10.1111/j.1462-2920.2006.01197.x
50. Lee CG, Watanabe T, Fujita Y, Asakawa S, Kimura M (2012) Heterotrophic growth of cyanobacteria and phage-mediated microbial loop in soil: examination by stable isotope probing (SIP) method. Soil Sci Plant Nutr 58:161–168. https://doi.org/10.1080/00380768.2012.658739
51. Ehleringer JR (1993) Carbon and water relations in desert plants: an isotopic perspective. Stable Isotopes and Plant Carbon-water Relations. Elsevier, pp 155–172. https://doi.org/10.1016/B978-0-08-091801-3.50018-0